Biased optimal guidance law with specified velocity rendezvous angle constraint

X. Xu[1,2,3]
xuxingyuan2003@126.com
Y. Liang[1]

[1] Information Engineering School
Henan University of Science and Technology
Luoyang
China,

[2] China Airborne Missile Academy
Luoyang
China

[3] Department of Automatic Control
Xi'an Jiao Tong University
Xi'an
China

ABSTRACT

In order to increase the effectiveness of interceptor missile, velocity rendezvous angle control is required in the terminal phase. The purpose of this paper is to obtain an optimal guidance law which can achieve specified velocity rendezvous angle as well as zero terminal miss distance. A biased optimal guidance law based on a simplified mathematical model is deduced for interceptors engaging against invasion aircraft. Different from previous literatures on this issue, the presented guidance law suitable for intercepting high-speed maneuvering target. Another advantage is, under centimeter level miss distance setting, the guidance law needs smaller guidance command near the terminal time, which can successfully avoid command saturation. Simulation results demonstrate the effectiveness of the presented guidance law.

1.0 INTRODUCTION

The main objective of traditional guidance laws is to produce zero terminal miss distance. Current applications demand additional terminal performance measures such as interception at a certain flight-path angle relative to the target's flight-path to increase warhead lethality. For example, kinetic kill vehicle (KKV) adopts the way of direct collision to destroy target, thus, control of

Paper No. 4390. Manuscript received 5 March 2015, revised version received 10 June 2015, accepted 25 June 2015.

https://doi.org/10.1017/S0001924000011258 Published online by Cambridge University Press

velocity rendezvous angle can increase its effectiveness. Guidance laws with angle constraint have been addressed in several contributions in the missile-guidance literature. Previous works on this issue can be classified into two categories: proportional navigation guidance (PNG) laws and optimal guidance laws (OGL).

PNG and its various variants[1,2] are very popular in engineering application primarily because of its efficiency. PNG employs feedback with a constant gain from the angular rate of the line of sight (LOS) to produce zero terminal miss distance. Such guidance laws are designed primarily for minimising the miss distance, and they are usually silent on impact angle constraints. However, within the PN philosophy, some variations have been proposed in the recent literature to cater for impact angle constraint as well[3]. Kim *et al*[3] proposed a time-varying biased PNG (BPNG) law to achieve a desired attitude angle of impact, which is an intuitive function composed of the state variables such as LOS angle, relative range, and flight-path angle. The authors of[4-6] proposed two-phase guidance schemes with terminal-angle constraint based on the conventional PNG laws. The guidance scheme suggested in Ref. 4 comprises PNG with a navigation gain $N < 2$ for covering all impact angles from 0 to $-\pi$ and PNG with $N = 2$ for intercepting stationary targets with a desired impact angle in surface-to-surface engagements. In Ref. 5, two-stage PNG law with different navigation constants to intercept stationary and nonstationary targets are designed using nonlinear engagement dynamics. These laws ensure that the lateral acceleration remains bounded even in the terminal phase. Using BPNG, Ref. 6 developed a similar two-phase scheme in which the missile follows BPNG with a constant bias for the initial homing phase and then switches to PNG (i.e., BPNG with zero bias) when the integral value of the bias satisfies a certain value. Because these two-phase guidance schemes only use the LOS rate information for the impact angle control, they can be applied to passive homing missile systems. Another guidance law, also based on nonlinear engagement dynamics but adopting a computational approach, defined by the particle-swarm-optimisation algorithm, is derived in Ref. 7. In Ref. 8, a BPNG law to intercept stationary targets is developed, which achieves the desired impact angle.

The requirement for better performance and optimal energy consumption has led to the development of modern guidance laws based on optimal control theory. For optimal guidance with angle control, the optimal control input is given by the solution to the linear quadratic optimal control problem. In Ref. 9, an optimal guidance law was derived for imposing a specified impact angle in a scenario in which a reentry vehicle pursues a fixed or slowly moving ground target. A sub-optimal angle control guidance law for interceptor having a varying velocity was proposed in Ref. 10. In Ref. 11, a linear quadratic angle constraint guidance law is presented, the guidance law introduce acceleration bounds into the cost function. An optimal guidance law for a missile with arbitrary-order dynamics launched against a stationary target was derived[12]. Reference 13 extends the same formulation by adopting a time-to-go weighted-energy cost function.

The majority of the guidance laws with angle constraint reviewed above are only suitable for stationary or slowly moving target (i.e., interceptor have a certain speed advantage relative to the target). For high speed maneuvering target, these guidance schemes require large guidance commands near the terminal time, thus, if the limitation of missile acceleration capability exists, a large miss distance is generated.

The aim of this paper is to carry out a more in-depth study of the previous optimal guidance law with velocity rendezvous angle constraint, make it suitable for intercepting high speed maneuvering target. And, under centimeter level miss distance setting, the guidance law can avoid command saturation near the terminal time.

https://doi.org/10.1017/S0001924000011258 Published online by Cambridge University Press

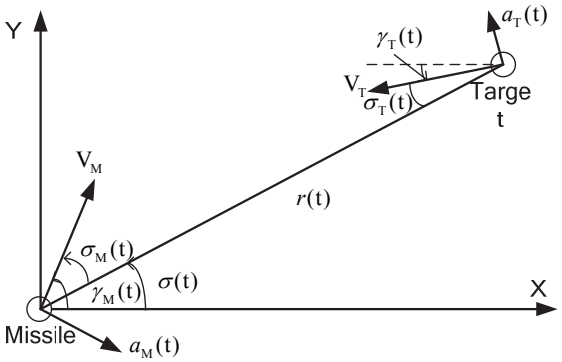


Figure 1. Geometry for derivation of the BPNG law.

2.0 PROBLEM STATEMENT

2.1 Brief introduction of BPNG law

BPNG law aroused a lot of people's interest. In this paper, we will contrast the performance of the presented biased optimal guidance law(BOGL) with BPNG law, and reveal their advantages and disadvantages. (Fig.1 near here)

As shown in Fig.1, V_M is the velocity of the missile, and a_M is the lateral acceleration of the missile. V_T is the velocity of the target, and a_T is the lateral acceleration of the target. $\gamma_M(t)$ and $\gamma_T(t)$ are the flight-path angles of adversaries, respectively. The relative range is $r(t)$. $\sigma(t)$ is the LOS angle. According to the above assumptions, BPNG law described in reference[8] can be expressed as:

$$u(t) = NV_M[\dot{\sigma}(t) - \dot{\sigma}_b(t)] \quad \ldots (1)$$

where N is the navigation constant, $\dot{\sigma}(t)$ is the LOS angle rate, and $\dot{\sigma}_b(t)$ denotes the biased term to control the impact angle. $\dot{\sigma}(t)$ and $\dot{\sigma}_b(t)$ can be expressed as:

$$\dot{\sigma}(t) = \frac{V_T \mathrm{Sin}\sigma_T(t) - V_M \mathrm{Sin}\sigma_M(t)}{r(t)} \quad \ldots (2)$$

$$\dot{\sigma}_b(t) = \frac{\eta V_M(\sigma_d - \sigma(t))}{Nr(t)\mathrm{Cos}\sigma_M(t)} \quad \ldots (3)$$

where, η is an arbitrary positive constant, and σ_d is the desired LOS angle at the time of rendezvous which can be replaced by the desired flight-path angle, γ_{Mf}.

As shown in Equation (1), the first term of Equation (1) is responsible for zero the miss distance, i.e., intercepting the target. The second term of Equation (1) is responsible for achieving a desired impact angle. Let $\dot{\sigma}_b = 0$, the BPNG law Equation (1) degenerates to the traditional PNG, i.e., no longer impose an intercept angle.

2.2 current model of BOGL

Figure 2 shows the planar motion engagement between a pursuer and an evader. The X-axis of the co-ordinate system is aligned with the initial LOS. The subscript P and E identify the pursuer (interceptor) and the evader (target). $\mathbf{V}_p$ and $\mathbf{V}_E$ are the constant velocities of the adversaries,

https://doi.org/10.1017/S0001924000011258 Published online by Cambridge University Press

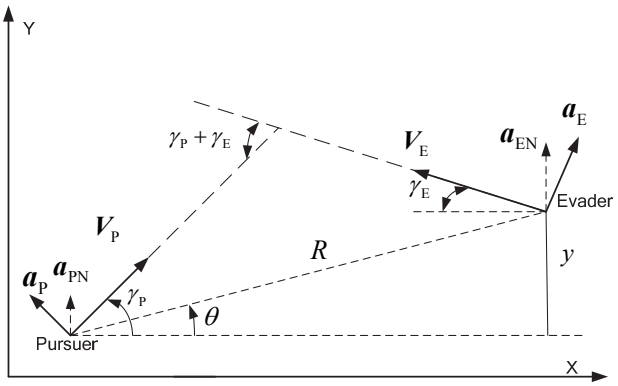


Figure 2. Geometry for derivation of the BOGL.

respectively. a_P and a_E are the lateral accelerations of the adversaries, respectively; The flight-path angles of the adversaries are denoted by γ_P ,γ_E , respectively; The relative range is R. θ is the angle between the LOS and the X-axis. The relative displacement between adversaries normal to the X-axis is y. The adversaries accelerations normal to the X-axis are denoted by a_{PN} and a_{EN} respectively; and, $a_{PN} = a_P \mathrm{Cos}\gamma_{P0}$, $a_{EN} = a_E \mathrm{Cos}\gamma_{E0}$. From the engagement geometry of Fig. 2, the motion equations can be expressed as:

$$\dot{\theta} = \frac{-V_P \mathrm{Sin}(\gamma_P - \theta) + V_E \mathrm{Sin}(\gamma_E + \theta)}{R} \quad \ldots (4)$$

$$\dot{R} = -V_P \mathrm{Cos}(\gamma_P - \theta) - V_E \mathrm{Cos}(\gamma_E + \theta) \quad \ldots (5)$$

$$\dot{\gamma}_E = a_E / V_E \quad \ldots (6)$$

$$\dot{\gamma}_P = a_P / V_P \quad \ldots (7)$$

Consider now the linear dynamical system characterised by the canonical equation:

$$\dot{\mathbf{x}}(t) = \mathbf{A}\mathbf{x}(t) + \mathbf{B}\mathbf{u}(t) \quad \ldots (8)$$

A simple case is considered in this paper, i.e., the pursuer is a lag-free system, and, neglecting its gravitational force. In this case:

$$a_P(t) = u(t) \quad \ldots (9)$$

If non-zero-lag dynamics were assumed for the pursuer, the processing method is similar. The assumption of lag-free dynamics is due to the simplicity and ease of presentation.

If the pursuer and evader deviations from the collision triangle (Fig. 2) are small in the terminal engagement, that is, the endgame is initiated with a collision triangle approximately satisfying the requirement on the velocity rendezvous angle ($\gamma_P + \gamma_E$), this initialisation can be performed by a midcourse guidance law. Then, the collision triangle is maintained. The assumption leads to

https://doi.org/10.1017/S0001924000011258 Published online by Cambridge University Press

the following linear model:

$$\begin{cases} \dot{x}_1 = x_2 \\ \dot{x}_2 = a_{\mathrm{E}}\mathrm{Cos}\,\gamma_{\mathrm{E}0} - a_{\mathrm{P}}\mathrm{Cos}\,\gamma_{\mathrm{P}0} \\ \dot{x}_3 = \dfrac{u_{\mathrm{E}} - a_{\mathrm{E}}}{\tau_{\mathrm{E}}} \\ \dot{x}_4 = a_{\mathrm{E}}/V_{\mathrm{E}} + a_{\mathrm{P}}/V_{\mathrm{P}} \end{cases} \quad \ldots (10)$$

Where $x_1 = y$. x_2 is the relative lateral velocity. x_3 is the lateral acceleration of the evader. In this paper, the evader maintain constant maneuver, therefore, $\dot{x}_3 = \dot{a}_E = 0$; x_4 is the required velocity rendezvous angle ($\gamma_P + \gamma_E$).
From Equations (6-10), one can obtain:

$$\mathbf{A} = \begin{bmatrix} 0 & 1 & 0 & 0 \\ 0 & 0 & \mathrm{Cos}\,\gamma_{\mathrm{E}0} & 0 \\ 0 & 0 & 0 & 0 \\ 0 & 0 & 1/\mathrm{V}_{\mathrm{E}} & 0 \end{bmatrix} \quad \ldots (11)$$

$$\mathbf{B} = \begin{bmatrix} 0 & -\mathrm{Cos}\,\gamma_{\mathrm{P}0} & 0 & 1/V_{\mathrm{P}} \end{bmatrix}^{\mathrm{T}} \quad \ldots (12)$$

$$\mathbf{x} = (x_1, x_2, x_3, x_4)^{\mathrm{T}} \quad \ldots (13)$$

Once the collision triangle is approximately reached and maintained (Fig. 2), the closing velocity between pursuer and evader can be assumed constant, and the time-to-go can be estimated as follow

$$t_g = -\frac{R}{\dot{R}} \quad \ldots (14)$$

3.0 BIASED OPTIMAL GUIDANCE LAW

3.1 Derivation of BOGL

The essence of the optimal guidance problem is to determine the guidance law $u(t)$ that minimises the quadratic performance index (or cost functional). In order to reduce energy consumption, the performance index to be minimised will be assumed to be given by Ref. 14.

$$J = \frac{1}{2}\mathbf{e}(t_f)^{\mathrm{T}}\mathbf{S}\mathbf{e}(t_f) + \frac{1}{2}\int_0^{t_f} \mathbf{u}^{\mathrm{T}}(\tau)\mathbf{R}\mathbf{u}(\tau)\,\mathrm{d}\,\tau \quad \ldots (15)$$

Where $\mathbf{e}(t_f) = \mathbf{x}(t_f) - \mathbf{x}_f$ is terminal error at the intercept time, t_f is the total flight time and $\mathbf{x}_f$ is the desired terminal state. The term $\mathbf{e}(t_f)^{\mathrm{T}}\mathbf{S}\mathbf{e}(t_f)$ is a penalty for deviations from the desired terminal state. The term $\mathbf{u}^{\mathrm{t}}(\tau)\mathbf{R}\mathbf{u}(\tau)$ discourages the use of large control effort. The control signal $\mathbf{u}(t)$ is obtained by minimising J, and $\mathbf{u}(t)$ is constrained by the weighting matrix $\mathbf{R}$. Here, $\mathbf{R} > 0$ and $\mathbf{S} \geq 0$ (semi-positive

https://doi.org/10.1017/S0001924000011258 Published online by Cambridge University Press

definite), and **S** is the final state error weighting matrix. There are four state variables in Equation (10), however, the guidance law in this paper only emphasises the states x_1 and x_4, that is, miss distance and velocity rendezvous angle. Thus, the system[14] can be reduced to a 2 × 1 vector variable using the transformation:

$$\mathbf{Z}(t) = \mathbf{D}\Omega(t_f, t)\mathbf{x}(t) \quad \ldots (16)$$

Here, $\mathbf{\Omega}(t_f,t)$ denotes the state transition matrix used to propagate the state from t to t_f, and **D** is a constant matrix:

$$\mathbf{D} = \begin{bmatrix} 1 & 0 & 0 & 0 \\ 0 & 0 & 0 & 1 \end{bmatrix} \quad \ldots (17)$$

$\mathbf{\Omega}(t_f,t)$ can be obtained by solving the homogeneous equation:

$$\dot{\mathbf{x}}(t) = \mathbf{A}\mathbf{x}(t) \quad \ldots (18)$$

From (18), one can obtain:

$$\mathbf{x}(t) = e^{\mathbf{A}t} = L^{-1}\{(s\mathbf{I} - \mathbf{A})^{-1}\}$$

$$= L^{-1}\begin{bmatrix} s & -1 & 0 & 0 \\ 0 & s & -\mathrm{Cos}\,\gamma_{E0} & 0 \\ 0 & 0 & s & 0 \\ 0 & 0 & -1/V_E & s \end{bmatrix}^{-1} = L^{-1}\begin{bmatrix} \frac{1}{s} & \frac{1}{s^2} & 0 & 0 \\ 0 & \frac{1}{s} & \frac{\mathrm{Cos}\,\gamma_{E0}}{s^2} & 0 \\ 0 & 0 & \frac{1}{s} & 0 \\ 0 & 0 & \frac{1}{s^2 V_E} & \frac{1}{s} \end{bmatrix} = \begin{bmatrix} 1 & t & 0 & 0 \\ 0 & 1 & t\,\mathrm{Cos}\,\gamma_{E0} & 0 \\ 0 & 0 & 1 & 0 \\ 0 & 0 & \frac{t}{V_E} & 1 \end{bmatrix} \quad \ldots (19)$$

Replace t with $t_f - t$, one can obtain the transition matrix:

$$\Omega(t_f, t) = e^{\mathbf{A}(t_f - t)} = \begin{bmatrix} 1 & t_f - t & 0 & 0 \\ 0 & 1 & (t_f - t)\mathrm{Cos}\,\gamma_{\mathrm{E0}} & 0 \\ 0 & 0 & 1 & 0 \\ 0 & 0 & \frac{t_f - t}{\mathrm{V_E}} & 1 \end{bmatrix} \quad \ldots (20)$$

From Equation (20), one can obtain:

$$\dot{\Omega}(t_f, t) = -e^{\mathbf{A}(t_f - t)}\mathbf{A} = -\Omega(t_f, t)\mathbf{A} \quad \ldots (21)$$

The 2 × 1 vector variable **Z**(t) represents the zero-effort miss and zero-effort velocity rendezvous angle. Then, the derivative with respect to time of the new state vector $\mathbf{Z}(t)$ is:

https://doi.org/10.1017/S0001924000011258 Published online by Cambridge University Press

$$\begin{aligned}\dot{\mathbf{Z}}(t) &= \mathbf{D}\dot{\Omega}(t_f,t)\mathbf{x}(t) + \mathbf{D}\Omega(t_f,t)\dot{\mathbf{x}}(t) \\ &= -\mathbf{D}\Omega(t_f,t)\mathbf{A}\mathbf{x}(t) + \mathbf{D}\Omega(t_f,t)(\mathbf{A}\mathbf{x}(t)+\mathbf{B}u(t)) = \mathbf{D}\Omega(t_f,t)\mathbf{B}u(t)\end{aligned} \quad \ldots (22)$$

From Equation (16), $\mathbf{Z}(t_f)$ can be expressed as:

$$\mathbf{Z}(t_f) = \mathbf{D}\Omega(t_f,t_f)\mathbf{x}(t) = \begin{bmatrix} x_1(t_f) \\ x_4(t_f) \end{bmatrix} \quad \ldots (23)$$

Here, $\mathbf{\Omega}(t_f,t_f) = \mathbf{I}$. Using the new variables $Z(t)$, the cost function, Equation (15)' can also be expressed as:

$$J = \frac{1}{2}\mathbf{Z}(t_f)^{\mathrm{T}}\mathbf{S}\mathbf{Z}(t_f) + \frac{1}{2}\int_0^{t_f}\mathbf{u}^{\mathrm{T}}(\tau)\mathbf{R}\mathbf{u}(\tau)\,\mathrm{d}\,\tau \quad \ldots (24)$$

In this paper, the following weights are chosen:

$$\mathbf{S} = \begin{bmatrix} a_1 & 0 \\ 0 & a_2 \end{bmatrix}, \mathbf{R} = [1] \quad \ldots (25)$$

where a_1, a_2 are nonnegative constants, and a_1, a_2 are selected by the guidance analyst[14]. Defining $\gamma_f = \gamma_P + \gamma_E$, $t_g = t_f - t$, the cost function (15) can also be expressed as:

$$J = \frac{a_1}{2}Z_1^2(t_f) + \frac{a_2}{2}[Z_2(t_f) - \gamma_f]^2 + \frac{1}{2}\int_0^{t_f}u(t)^2\mathrm{d}t \quad \ldots (26)$$

The zero-effort miss and velocity rendezvous angle varies in accordance with the following equation:

$$\dot{\mathbf{Z}}(t) = \mathbf{D}\Omega(t_f,t)\mathbf{B}u(t) = \begin{bmatrix} -t_g\mathrm{Cos}\gamma_{\mathrm{P0}} \\ 1/V_{\mathrm{P}} \end{bmatrix}u(t) \quad \ldots (27)$$

The projection of the pursuer's command acceleration in the direction perpendicular to the initial LOS is $u = u_p\mathrm{Cos}\gamma_{\mathrm{PO}}$. The pursuer's velocity components on the initial LOS is $\mathrm{V}'_p = \mathrm{V}_p\mathrm{Cos}\gamma_{\mathrm{PO}}$. Then, Equation (27) simplifies to:

$$\begin{cases} \dot{Z}_1 = -t_g u \\ \dot{Z}_2 = u/\mathrm{V}'_{\mathrm{P}} \end{cases} \quad \ldots (28)$$

According to optimal control theory, through minimising cost function (26), one can obtain biased optimal guidance law:

$$u^*(t) = a_1 t_g Z_1(t_f) - \frac{a_2}{\mathrm{V}'_{\mathrm{P}}}[Z_2(t_f) - \gamma_f] \quad \ldots (29)$$

Substituting Equations (29) into (28), and integrating from t to t_f with boundary conditions from (23), the closed-form trajectory solutions of $\boldsymbol{Z}_1(t_f)$ and $\boldsymbol{Z}_2(t_f)$ are obtained, respectively.

$$Z_1(t_f) = Z_1(t) - a_1 Z_1(t_f)\frac{t_g^{\,3}}{3} + \frac{a_2}{\mathrm{V}'_{\mathrm{P}}}[Z_2(t_f) - \gamma_f]\frac{t_g^{\,2}}{2} \quad \ldots (30)$$

$$Z_2(t_f) = Z_2(t) + \frac{a_1}{\mathrm{V}'_{\mathrm{P}}}Z_1(t_f)\frac{t_g^{\,2}}{2} - \frac{a_2}{\mathrm{V}'_{\mathrm{P}}}[Z_2(t_f) - \gamma_f]t_g \quad \ldots (31)$$

https://doi.org/10.1017/S0001924000011258 Published online by Cambridge University Press

Solving for $Z_1(t_f)$ and $Z_2(t_f)$ and substituting the solution into Equation (29) yields the following optimal controller:

$$u^*(t) = \frac{\mathrm{C}_1}{t_g^2} Z_1(t) + \mathrm{C}_2 \frac{\mathrm{V}_\mathrm{P}^{'}}{t_g} [Z_2(t) - \gamma_f] \quad \ldots (32)$$

where:

$$\mathrm{C}_1 = \frac{3a_1 t_g^3}{3 + a_1 t_g^3} + \frac{a_2 f_3(t_g) f_2(t_g) t_g^2}{f_1(t_g) + V_\mathrm{P}^{'2}} \quad \ldots (33)$$

$$\mathrm{C}_2 = \frac{a_2 f_3(t_g) t_g}{f_1(t_g) + V_\mathrm{P}^{'2}} \quad \ldots (34)$$

$$f_1(t_g) = \frac{a_2(a_1 t_g^4 + 12 t_g)}{4(3 + a_1 t_g^3)} \quad \ldots (35)$$

$$f_2(t_g) = \frac{3a_1 t_g^2}{2(3 + a_1 t_g^3)} \quad \ldots (36)$$

$$f_3(t_g) = \frac{a_1 t_g^3 - 6}{2(3 + a_1 t_g^3)} \quad \ldots (37)$$

As mentioned above, through the new state vector $\boldsymbol{Z}(t)$, the order of the problem is reduced. In addition, the two variables of $\boldsymbol{Z}(t)$ have other important physical meaning. $Z_1(t)$ is known as the zero-effort miss distance; and $Z_2(t)$ is known as zero-effort velocity rendezvous angle. Then, $Z_2(t) - \gamma_f$ can be denoted as the zero-effort angle error. $Z_1(t)$ and $Z_2(t)$ can be expressed as:

$$Z_1(t) = y + \dot{y} t_g + a_\mathrm{E} \mathrm{Cos}\gamma_\mathrm{E} t_g^2 / 2 \quad \ldots (38)$$

$$Z_2(t) = t_g a_\mathrm{E} / V_\mathrm{E} + \gamma_\mathrm{E} + \gamma_\mathrm{P} \quad \ldots (39)$$

Under the assumption of small flight path-angle, and the pursuer can measure the LOS angle $\theta(t)$, the relative displacement y can be approximated by:

$$y \approx \theta R \quad \ldots (40)$$

Then, Equation (38) can be expressed as:

$$Z_1(t) = -\dot{\theta}\dot{R} t_g^2 + a_\mathrm{E} t_g^2 / 2 \quad \ldots (41)$$

https://doi.org/10.1017/S0001924000011258 Published online by Cambridge University Press

3.2 Relationship between BOGL and other guidance laws

As shown in Equation (29), the first term of Equation (29) is responsible for zero the miss distance, i.e., intercepting the evader. The second term of Equation (29) is responsible for zero the velocity rendezvous angle error, i.e., achieving a desired velocity rendezvous angle. By choosing $a_2 \to 0$, the optimal guidance law degenerate to the OGL presented in Ref. 15, i.e., no longer impose an intercept angle. Also, choosing $a_1 \to \infty$ indicates the guidance law further degenerates to the well-known augmented proportional navigation (APN) guidance law, and the navigation gain is three:

$$\begin{cases} \lim\limits_{\substack{a_1\to\infty \\ a_2\to 0}} \mathrm{C}_1 = 3 \\ \lim\limits_{\substack{a_1\to\infty \\ a_2\to 0}} \mathrm{C}_2 = 0 \end{cases} \quad \ldots (42)$$

For achieving a specified velocity rendezvous angle, $a_1 \to \infty$ and a finite a_2 are required, in this case:

$$\begin{cases} \lim\limits_{a_1\to\infty} \mathrm{C}_1 = 3 + \dfrac{3a_2 t_g}{a_2 t_g + 4V_{\mathrm{P}}^{'2}} \\ \lim\limits_{a_1\to\infty} \mathrm{C}_2 = \dfrac{2a_2 t_g}{a_2 t_g + 4V_{\mathrm{P}}^{'2}} \end{cases} \quad \ldots (43)$$

By choosing $a_1 \to \infty$ and $a_2 \to \infty$, one can obtain:

$$\begin{cases} \lim\limits_{\substack{a_1\to\infty \\ a_2\to\infty}} \mathrm{C}_1 = 6 \\ \lim\limits_{\substack{a_1\to\infty \\ a_2\to\infty}} \mathrm{C}_2 = 2 \end{cases} \quad \ldots (44)$$

Substituting Equation (44) into Equation (32), one can obtain:

$$u^*(t) = \frac{6}{t_g^2} Z_1(t) + 2\frac{V_{\mathrm{P}}^{'}}{t_g}[Z_2(t) - \gamma_f] \quad \ldots (45)$$

Equation (45) indicates the BOGL is similar to the optimal APN and the PN cases when $a_1 \to \infty$ and $a_2 \to \infty$. Moreover, the gain associated with the zero-effort miss is multiplied by a factor of 2 compared with the optimal PN and APN cases, which might result in an increased sensitivity to measurement noise[14].

4.0 NUMERICAL ANALYSIS

4.1 BOGL performance

In order to demonstrate the performance of the proposed BOGL, nonlinear simulations are performed. The initial conditions for the nonlinear simulation are given in Table 1.

Figure 3 denotes the trajectories of the adversaries with various velocity rendezvous angles. Figure 4 denotes optimal guidance commands corresponding to Fig. 3. One can see from Fig. 4, the guidance commands for various velocity rendezvous angles are not large near the terminal

https://doi.org/10.1017/S0001924000011258 Published online by Cambridge University Press

time, which can avoid command saturation. Theoretically speaking, the proposed BOGL can achieve any velocity rendezvous angles. However, large angle will lead to large lateral acceleration requirement during the flight. Therefore, it is necessary to select appropriate initial heading angle of the interceptor to avoid this situation. The change trends of zero-effort miss $Z_1(t)$ and zero-effort velocity rendezvous angles $Z_2(t)$ are shown in Figs 5 and 6. One can see, zero-effort miss tend to zero, and zero-effort angles tend to the desired velocity rendezvous angles.

The magnitude of a_1 and a_2 are to exercise a great influence on guidance performance, and there are a more in-depth discussion in section 3.2. Figs 7 and 8 show the change trends of navigation gains C_1 and C_2 with a_2, respectively.

Table 1
Initial conditions for BOGL law simulation

Parameter	value
Pursuer initial position	(0m, 0m)
Evader initial position	(10,000m, 0m)
Pursuer flight velocity	1,500ms^{-1}
Evader flight velocity	1,500ms^{-1}
Pursuer initial flight path angle	0°
Evader initial flight path angle	0°
Acceleration of Evader	50ms^{-2}
Mass distance	0·1m
Constant coefficient a_1	10^5
Constant coefficient a_2	10^8

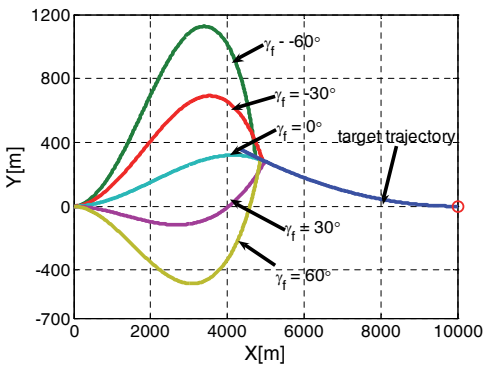


Figure 3. Trajectories of adversaries using BOGL.

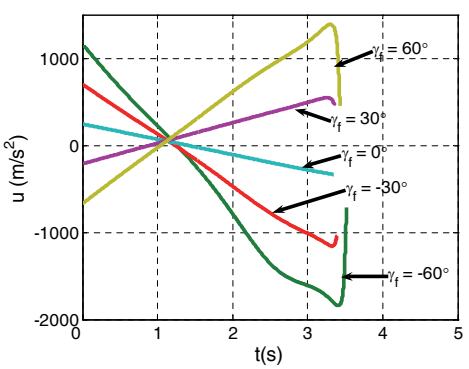


Figure 4. Optimal guidance commands for various velocity rendezvous angles.

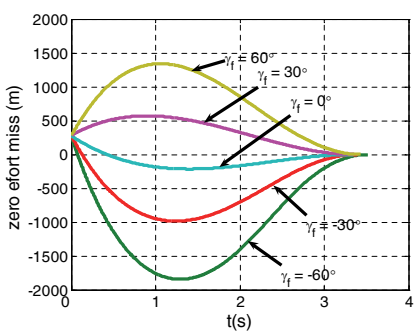


Figure 5. Histories of the zero-effort miss.

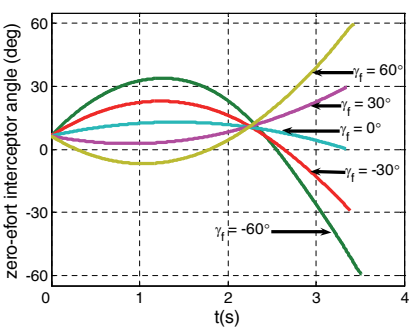


Figure 6. Histories of the zero-effort velocity rendezvous angles.

https://doi.org/10.1017/S0001924000011258 Published online by Cambridge University Press

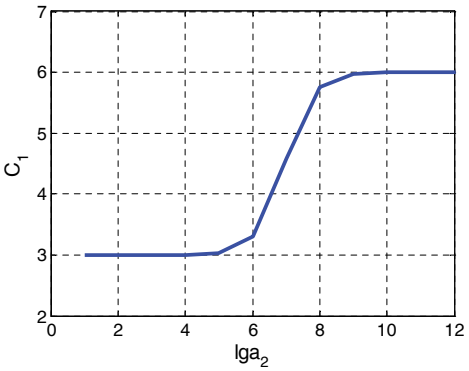


Figure 7. Change trends of C_1 vs lg a_2 ($a_1 = 10^5$, $V'_p = 1{,}500\text{ms}^{-1}$).

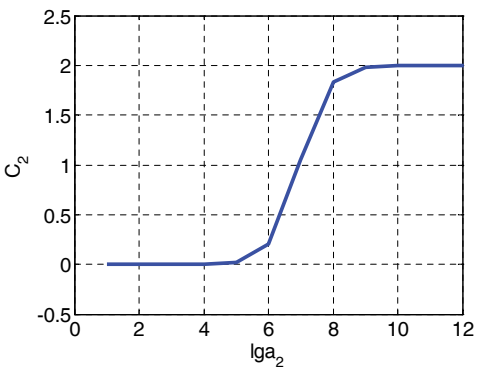


Figure 8. Change trends of C_2 vs lg a_2 ($a_1 = 10^5$, $V'_p = 1{,}500\text{ms}^{-1}$).

4.2 BPNG performance

In order to reveal the advantages and disadvantages of the proposed law with BPNG, nonlinear simulations of BPNG are also presented. Initial parameters for BPNG law simulation is shown in Table 2. In Tables 1 and 2, some parameters are identical, such as, initial positions of pursuer and evader, initial flight path angles of pursuer and evader, pursuer velocity etc,. However, the evader velocities are different in the two tables. The reason is that BPNG requires pursuer has a velocity advantage relative to target, i.e., $V_p > V_p^{(8)}$. In addition, the miss distance setting is different.

Figure 9 denotes the trajectories for various impact angles using BPNG. Figure 10 denotes BPNG guidance commands corresponding to Fig. 9. One can see, BPNG can simultaneously control miss distance and flight-path angle. When a large impact angle is imposed, the guidance commands of BPNG tend to diverge (Fig. 10).

Compare Fig. 4 with Fig. 10, one can see, the guidance commands of the proposed law tend to convergence near rendezvous point (Fig. 4), and the guidance commands of BPNG tend to diverge (Fig. 10). More importantly, the miss distance setting of the proposed law is 0·1m, and the velocities of the adversaries are all $1{,}500\text{ms}^{-1}$, i.e., the interceptor has not velocity advantage relative to the target. Yet the miss distance setting of the BPNG is 10m. If smaller miss distance setting and higher target velocity impose to the BPNG, the guidance commands near rendezvous point will tend to infinity, which will definitely result in command saturation. All these show that BPNG law is not

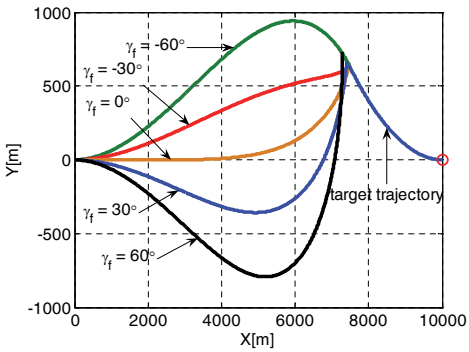


Figure 9. Interceptor and target's flight path using BPNG law.

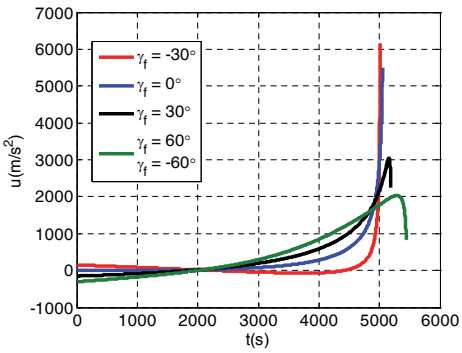


Figure 10. The guidance commands of the BPNG law.

https://doi.org/10.1017/S0001924000011258 Published online by Cambridge University Press

Table 2
Initial parameters for BPNG law simulation

parameter	value
Miss distance	10m
Constant N	4·0
Constant η	1·3
Pursuer flight velocity V_M	1,500ms^{-1}
Evader initial velocity V_T	500ms^{-1}
Acceleration of Evader a_T	50ms^{-2}
Pursuer initial flight path angle γ_{M0}	0°
Evader initial flight path angle γ_{T0}	0°
Evader initial position	(10,000m, 0m)
Pursuer initial position	(0m, 0m)

suitable for intercepting high speed maneuvering target. The most attractive feature of BPNG is the ease of implementation and its efficiency. Also, BPNG needs not to estimate time-to-go.

Although BPNG has not good enough performance against high speed target, BPNG can be performed as a midcourse guidance law. When a collision triangle is approximately achieved (Fig.2), the proposed BOGL comes into effect. The reason is that the BOGL is obtained under the assumption that the endgame is initiated with a collision triangle approximately satisfying the requirement on the velocity rendezvous angle ($\gamma_P + \gamma_E$).

4.3 Miscellanea

In this paper, pursuer and evader are considered as geometric points, and a guidance law is presented. The influence of the uncertainties that are produced by aerodynamics does not take into account, these uncertainties include pursuer axial speed variation, aerodynamic orientation angles, and surface deflections etc. In addition, in order to apply the guidance law, the pursuer is required to obtain necessary information, such as $Z_1(t)$, $Z_2(t)$, t_g, $\boldsymbol{V}_p$ etc. Tracking and sensor lags are also not considered. These issues can be regarded as another special subject to study. Many research efforts have been reported in the literature to estimate the parameter deviations[16].

For missile interception scenarios, head-on and tail-chase scenarios are well-known interception problems. In head-on interception, the adversaries fly toward each other, the closing velocity is very high. Thus, this scenario requires the pursuer subsystems could detect the target from a large distance and have very fast response time. In tail-chase interception, the pursuer chases the evader, the closing velocity significantly reduced. However, the tail-chase scenario requires the pursuer have a velocity advantage relative to the evader. In general, if the pursuer can successfully hit a high speed target, there will be better performance against low velocity target. For the above reasons, only head-on interception is showed in the simulation results.

5.0 CONCLUSIONS

In this paper, an optimal velocity rendezvous angle control guidance law has been derived. The guidance law ensures optimal energy consumption, avoid command saturation in terminal engagement. Nonlinear simulation results show that the proposed BOGL produce good performance

https://doi.org/10.1017/S0001924000011258 Published online by Cambridge University Press

under centimeter level miss distance setting. In the simulation process, the adversaries have similar velocity setting, and the maneuverability of the target is considered, all these show that the BOGL suitable for interceptor high-speed maneuvering target. Moreover, although the BOGL is obtained under the assumption that the adversaries deviation from the collision triangle are small, however, simulation results show that the law still has good performance when the deviations are large. In application of the proposed BOGL, information such as the current position, LOS angle, and velocity can be provided by a built-in inertial navigation system and a normal seeker.

More research is needed in the future work. The performance of the BOGL is critically dependent on the accuracy of time-to-go estimates, better time-to-go estimate method should be research. In real situation, the velocity of the adversaries is time-varying. Hence, the influence of the varying velocity will be studied in the future. And, the effect of autopilot lags is also our future works.

REFERENCES

1. ZARCHAN, P. *Tactical And Strategic Missile Guidance*, 5th ed (Progress in Astronautics and Aeronautics), AIAA, 5th ed, 2007.
2. SIOURIS, G.M. *Missile Guidance and Control Systems*, Springer, New York, US, 2003.
3. KIM, B.S., LEE, J.G. and HAN, S.H. Biased PNG law for impact with angular constraint, *IEEE Transactions on Aerospace and Electronic Systems*, 1998, **34**, (1), pp 277-288.
4. RATNOO, A and GHOSE, D. Impact angle constrained interception of stationary targets, *J Guidance, Control and Dynamics*, 2008, **31**, (6), pp 1816-1821.
5. RATNOO, A and GHOSE, D. Impact angle constrained guidance against nonstationary non-maneuvering targets, *J Guidance, Control and Dynamics*, 2010, **33**, (1), pp 269-275.
6. ERER, K.S. and MERTTOPÇUO, L.O. Indirect impact-angle-control against stationary targets using biased pure proportional navigation, *J Guidance, Control and Dynamic*, 2012, **35**, (2), pp 700-703.
7. SANG, D., MIN, B.M. and TAHK, M.J. Impact angle control guidance law using Lyapunov function and PSO method, Proc. of the SICE annual conference, TAKAMATSU, JP, 2007.
8. JEONG, S.K., CHO, S.J. and KIM, E.G. Angle constraint biased PNG, Proc of the 5th asian control conference, Melbourne, Victoria, Australia, 2004.
9. KIM, M and GRIDER, K.V. Terminal guidance for impact attitude angle constrained flight trajectories, IEEE Transactions on Aerospace and Electronic Systems, 1973, **AES-9**, (6), pp 852-859.
10. TAUB, I. Interceptor angle guidance under time varying speed, AIAA guidance, navigation, and control conference, 5-9 January, Kissimmee, Florida, US, 2015.
11. TAUB, I and SHIMA, T. Interceptor angle guidance under time varying acceleration bounds, *J Guidance, Control and Dynamic*, 2013, **36**, (3), pp 686-699.
12. RYOO, C.K., CHO, H and TAHK, M.J. Optimal guidance laws with terminal impact angle constraint, *J Guidance, Control and Dynamics*, 2005, **28**, (4), pp 724-732.
13. RYOO, C.K., CHO, H and TAHK, M.J. Time-to-go weighted optimal guidance with impact angle constraints, *IEEE Transactions of Control Systems*, 2006, **14**, (3), pp 483-492.
14. SHAFERMAN V and SHIMA, T. Linear quadratic guidance laws for imposing a terminal intercept angle, *J Guidance, Control and Dynamic*, 2008, **31**, (5), pp 1400-1412.
15. BEN-ASHER, J.Z. and YAESH, I. Advances in missile guidance theory, *Progress in Astronautics and Aeronautics*, AIAA, Reston, VA, US, 1998, (180), pp 25-90.
16. MARTINEZ-VAL, R. and PEREZ, E. Aeronautics and astronautics: recent progress and future trends, Proc. *IMechE, Part C: Journal of Mechanical Engineering Science*, 2009, **223**, (C12), pp 2767-2820.

https://doi.org/10.1017/S0001924000011258 Published online by Cambridge University Press